Kinetic modelling of primary and secondary interstellar oxygen atom fluxes in the heliosphere

I I Balyukin[1,2], V V Izmodenov[1,2,3], O A Katushkina[1] and D B Alexashov[1,3]

[1]Space Research Institute of Russian Academy of Sciences, Profsoyuznaya Str. 84/32, Moscow, 117335, Russia
[2]Lomonosov Moscow State University, GSP-1, Leninskie Gory, Moscow, 119991, Russia
[3]A.Ishlinsky Institute for Problems in Mechanics, prosp. Vernadskogo 101, block 1, Moscow, 119526, Russia

E-mail: balyukin.ii@gmail.com

Abstract. The interstellar neutral (ISN) oxygen atoms penetrate into the heliosphere from the Local Interstellar Medium (LISM). Oxygen atoms that directly penetrate into the heliosphere are called primary, while secondary oxygen population is formed near the heliopause due to the process of charge exchange of interstellar oxygen ions with hydrogen atoms and its existence in the heliosphere was previously predicted theoretically (Izmodenov et al., 1997, 1999, 2004). In this work we study the distribution of both primary and secondary oxygen atoms in the heliosphere and its fluxes at 1 AU.

The analysis of the distribution of ISN O atoms in the heliosphere is only possible in the frame of a model that takes into account both filtration of the primary and origin of the secondary interstellar oxygen in the region of interaction of the solar wind (SW) with the LISM, as well as a detailed simulation of the motion of interstellar atoms inside the heliosphere. This simulation should take into account the temporal and heliolatitudinal dependences of ionization, the process of charge exchange with SW protons and the effect of the solar gravitational attraction. This paper presents the results of modelling ISN O atoms inside the heliosphere based on a new three-dimensional kinetic-MHD model of the SW interaction with the LISM (Izmodenov and Alexashov, 2015). Oxygen atoms are of a particular interest because they are strongly coupled with the protons through the charge exchange process and due to the fact that the fluxes of interstellar oxygen are directly measured by the Interstellar Boundary Explorer (IBEX). The first quantitative measurements of the interstellar heavy neutral atoms (O and Ne) obtained on the IBEX spacecraft were presented in (Park et al., ApJS, 2015). Qualitative analysis of these data shows that the secondary component of the interstellar oxygen atoms was also measured along with the primary interstellar atoms.

1. Introduction

Our Solar System is moving through the Local Interstellar Cloud (LIC) with the bulk velocity about $26\,km\,s^{-1}$ (see, e.g., McComas et al. [1]). The solar wind (SW) interacts with the ionized component of Local Interstellar Medium (LISM), which is surrounding our solar system, and the SW/LISM interaction region (heliospheric interface) is formed. It consists of two shocks, termination shock (TS) and bow shock (BS), and a tangential discontinuity – heliopause (HP). The region between the shocks is called a heliosheath.

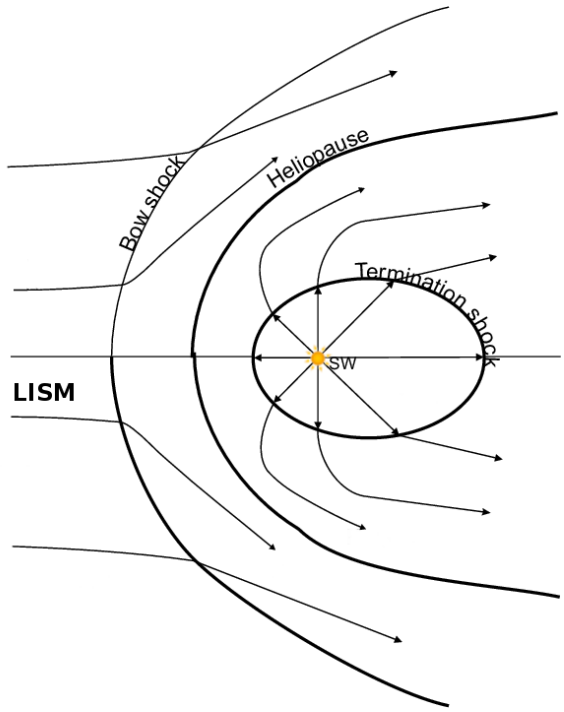

Figure 1. Qualitative picture of the SW/LISM interaction region: 2 shock waves (termination shock, bow shock) and tangential discontinuity (heliopause).

The LISM contains neutral elements such as H, He, O and Ne that have a large mean free path (by the process of charge exchange) that is comparable (for H and O) or larger (for He and Ne) than the character size of the heliosphere, so these atoms can penetrate into the heliosphere due to the relative motion of the Sun and LISM. In this work we study the distribution of the interstellar neutral (ISN) oxygen atoms in the heliosphere and particularly its fluxes at Earth's orbit.

Oxygen is the third element (after H and He) by its cosmic abundance in the LISM: $n_{O,LISM} = 0.78 \times 10^{-4} cm^{-3}$ (e.g., Izmodenov et al., [2]). Charge exchange cross section of interstellar oxygen atoms with protons is quite large (Izmodenov et al., [3]). Therefore, oxygen distribution inside the heliosphere is substantially modified by charge exchange in the heliospheric interface. For theoretical consideration it is convenient to divide interstellar oxygen atoms in two populations: primary and secondary. Atoms that directly penetrate into the heliosphere from the LISM we call primary. The secondary atoms are created via charge exchange between the oxygen ions and hydrogen atoms ($O^+ + H \rightarrow O + H^+$) in the region of disturbed interstellar plasma outside of the heliopause. Parameters of the secondary atoms depend on the local plasma properties in the region of their creation. Therefore, secondary oxygen atoms have smaller velocity and larger temperature compared to the primary ones because the interstellar plasma is decelerated and heated near the heliopause. Existence of the secondary oxygen population was theoretically predicted by Izmodenov et al. [3]. Filtration of interstellar oxygen at the heliospheric interface was also studied by Izmodenov et al. [4, 2].

Until recently, the interstellar neutral oxygen was measured only indirectly in the form of pick-up ions (Geiss et al., [5]) and anomalous cosmic rays (Cummings et al., [6]). First direct measurements of interstellar heavy neutral atoms (oxygen and neon) fluxes were performed by an Interstellar Boundary Explorer (IBEX) spacecraft. Qualitative analysis of this data performed by Park et al. [7] shows that the secondary component of the interstellar oxygen was detected for the first time. It is shown by Park et al. [7] that a sky map of interstellar heavy neutral atom fluxes contains a specific feature, which is called an extended "tail", associated with a contribution of secondary oxygen atoms.

In this work we perform a detailed numerical modelling of the ISN O fluxes at 1 AU. We consider both primary and secondary O atoms. Our model takes into account dynamics of atoms near the Sun under an influence of the solar gravitational force and local ionization processes as well as perturbations of the oxygen distribution at the heliospheric boundary.

The paper is organized as follows. In Section 2, the mathematical formulation of the problem and a detailed description of the model are provided. Section 3 describes the method of calculation of the model fluxes at 1 AU. Section 4 presents the results of the model numerical calculations. Finally, Section 5 is an overall summary of our work with conclusions.

2. Model of the ISN O distribution

In this section we introduce a brief description of the kinetic model of the ISN O distributions that we used in our calculations. Kinetic approach is only valid for description of the ISN atoms because of their large mean free path comparable to a character distance of the heliosphere. This model was proposed by Izmodenov et al. [8] and previously applied for modelling of He and H fluxes by Katushkina et al. [9] and Katushkina et al. [10], respectively. It is a 3D time-dependent version of the classical hot model (see, e.g., Izmodenov et al. [11]) with a specific boundary conditions at 90 AU based on the results of a global self-consistent model of the SW/LISM interaction. The numerical calculations were performed separately for the primary (O_{pr}) and secondary (O_{sec}) populations of the interstellar oxygen atoms.

2.1. Kinetic model

Kinetic approach is based on the conception of the velocity distribution function. Distribution of the ISN O atoms is described by a kinetic equation:

$$\frac{\partial f(\mathbf{r},\mathbf{v},t)}{\partial t} + \mathbf{v}\cdot\frac{\partial f(\mathbf{r},\mathbf{v},t)}{\partial \mathbf{r}} + \frac{\mathbf{F}}{m}\cdot\frac{\partial f(\mathbf{r},\mathbf{v},t)}{\partial \mathbf{v}} = -\beta(\mathbf{r},t)\cdot f(\mathbf{r},\mathbf{v},t), \quad (1)$$

where $f(\mathbf{r},\mathbf{v},t)$ is the velocity distribution function of O atom, $\mathbf{v}$ – individual velocity of an atom, t – time, m – mass of an atom, $\beta(\mathbf{r},t)$ – effective ionization rate. $\mathbf{F}$ is the force acting on each atom in the heliosphere. In general case, this force is the sum of a solar gravitational force $\mathbf{F}_g$ and a solar radiative repulsive force $\mathbf{F}_{rad}$, but we assume that $\mathbf{F}_{rad}$ is negligible ($\mu = |\mathbf{F}_{rad}|/|\mathbf{F}_g| \ll 1$) due to the O atom solidity. In view of this assumption resulting force $\mathbf{F}$ can be written in this form:

$$\mathbf{F} = \mathbf{F}_g = -m\frac{GM_\odot}{r^2}\frac{\mathbf{r}}{r},\ r = |\mathbf{r}|,$$

where G – gravitational constant, and $M_\odot$ – mass of the Sun.

Right side of the equation 1 represents the loss of atoms due to following processes: charge exchange on the SW protons ($O + H^+ \rightarrow O^+ + H$) and photoionization ($O + h\nu \rightarrow O^+ + e$). An electron impact ionization is not taken into account in our study because it is negligibly small as shown by Bzowski et al. [12]. Thus, the effective ionization rate can be written as: $\beta(\mathbf{r},t) = \beta_{ex}(\mathbf{r},t) + \beta_{ph}(\mathbf{r},t)$, where β_{ex} and β_{ph} are the rates of the charge exchange and photoionization, respectively.

Parameters β_{ex} and β_{ph} decrease with the distance r from the Sun $\propto 1/r^2$ in the region between the Sun and TS, since these values are proportional to the density of the SW protons and flux of the solar photons, respectively. Hereby, coefficient $\beta(\mathbf{r},t)$ can be rewritten as it follows:

$$\beta(\mathbf{r},t) = \beta^E(t,\lambda)\cdot\left(\frac{r_E}{r}\right)^2,\ \beta^E(t,\lambda) = \beta^E_{ex}(t,\lambda) + \beta^E_{ph}(t,\lambda),$$

where $r_E = 1$ AU, subscript "E" means that the value is taken at r_E. In general case, parameter $\beta^E(t,\lambda)$ depends on a time t and heliolatitude λ. We performed calculations with different ionization models ($\beta^E(t,\lambda)$; $\beta^E(t)$; $\beta^E = const$) and found that temporal and heliolatitudinal

dependences of ionization rate has no qualitative effect on flux maps. Thus, in calculations we used a simplified model with constant ionization rate $\beta^E = 5.2 \times 10^{-7} s^{-1}$ (this value is obtained by averaging of the total in-ecliptic ionization rates from 2009 to 2011 presented by Bzowski et al. [12]).

2.2. Method of characteristics

The kinetic equation (1) is a linear partial differential equation that can be solved by a method of characteristics. A characteristic is a curve in the phase space $\mathbb{R}^6$ of coordinates and velocities and it is defined by the following equations:

$$\begin{cases} d\mathbf{r}/dt = \mathbf{v}, \\ d\mathbf{v}/dt = \mathbf{F}/m. \end{cases} \tag{2}$$

Along this characteristic the velocity distribution function $f(\mathbf{r}, \mathbf{v}, t)$ must satisfy the following equation:

$$\frac{df(\mathbf{r}, \mathbf{v}, t)}{dt} = -\beta(\mathbf{r}, t) \cdot f(\mathbf{r}, \mathbf{v}, t),$$

and the solution of that equation can be written in the following form:

$$f(\mathbf{r}, \mathbf{v}, t) = f_s(\mathbf{r}_s, \mathbf{v}_s) \cdot e^{-I},\ I = \int_{t_s}^{t} \beta^E(t, \lambda) \cdot \left(\frac{r_E}{r}\right)^2 dt,$$

where $f_s(\mathbf{r}_s, \mathbf{v}_s)$ is the velocity distribution function of the O atoms at the outer boundary of the computational domain that is a Sun-centered sphere with radius $R_s = 90$ AU; $\mathbf{r}_s$, $\mathbf{v}_s$, t_s – position, velocity and moment of the time respectively when the atom crossed the outer boundary and enters the computational domain; I is a loss integral due to ionization processes. The integration is performed along the atom's trajectory that satisfies the system of equations (2) of the characteristic curve.

By solving the kinetic equation (1) with a specific boundary condition $f_s(\mathbf{r}_s, \mathbf{v}_s)$ we can find the value of the velocity distribution function everywhere in the computational domain. In the section below we describe a boundary conditions that are used in our modelling.

2.3. Boundary conditions

For the primary and secondary components of neutral oxygen atoms we used boundary condition on a sphere with radius $R_s = 90$ AU. To calculate the flow of oxygen atoms at this sphere we apply a new state-of-art kinetic-MHD model of the solar wind interaction with the LISM (hereinafter we call it a "global model"; this model is described in detail in the work of Izmodenov and Alexashov, [13]). In the present work parameters of the LISM were taken from the results of Witte et al. [14] that is based on Ulysses data: $V_{LISM} = 26.4\, km\, s^{-1}$; the LISM temperature $T_{LISM} = 6530 K$; direction of the interstellar wind in the ecliptic (J2000) coordinates – longitude $\lambda_{LISM} = 75.4°$ and latitude $\beta_{LISM} = -5.2°$; direction of the interstellar magnetic field in the ecliptic (J2000) coordinates – longitude 62.49° and latitude −20.79°. $\mathbf{B}_{LISM}\mathbf{V}_{LISM}$-plane coincides with the Hydrogen Deflection Plane (HDP) first proposed by Lallement et al. [15]. Hereinafter we also use a term "upwind" direction, which is defined by the opposite to the $\mathbf{V}_{LISM}$ vector direction, i.e., $(\lambda,\ \beta)_{upwind} = (255.4°,\ 5.2°)$.

At first, let us introduce a coordinate system, which we use to describe a boundary velocity distribution function: Z-axis pointing toward the "upwind" direction; XZ-plane (so-called BV-plane) is defined by two vectors – interstellar magnetic field vector $\mathbf{B}_{LISM}$ and the velocity vector of the interstellar wind $\mathbf{V}_{LISM}$; positive direction of X-axis have been chosen in the way

that z-component of the $\mathbf{B}_{LISM}$ has a negative value, i.e., $(\mathbf{B}_{LISM})_x < 0$; Y-axis complements the left-handed triplet.

Then we calculated the following parameters of the O_{pr} and O_{sec} on the boundary sphere using the global model:

- zero velocity distribution function moment – number density n_O:

$$n_O(\mathbf{r}_s) = \int f(\mathbf{r}_s, \mathbf{v}) \cdot d\mathbf{v}; \tag{3}$$

- first velocity distribution function moments – components of bulk velocity (V_x, V_y, V_z):

$$V_i(\mathbf{r}_s) = \frac{1}{n_O(\mathbf{r}_s)} \cdot \int f(\mathbf{r}_s, \mathbf{v}) \cdot v_i \cdot d\mathbf{v}; \tag{4}$$

- second velocity distribution function moments – kinetic temperatures (T_x, T_y, T_z):

$$T_i(\mathbf{r}_s) = \frac{m_O}{n_O(\mathbf{r}_s) k_B} \cdot \int f(\mathbf{r}_s, \mathbf{v}) \cdot (V_i(\mathbf{r}_s) - v_i)^2 \cdot d\mathbf{v}. \tag{5}$$

In formulas (3, 4, 5) we use the following notations: $i \in \{x, y, z\}$, k_B – Boltzmann constant, $d\mathbf{v} = dv_x \cdot dv_y \cdot dv_z$ and integration performed all over the velocity phase space $\mathbf{v} = (v_x, v_y, v_z) \in \mathbb{R}^3$. Parameters ($n_O$, V_i, T_i) – velocity distribution function moments – depend on a position of the atom on a boundary sphere. Table 1 presents values of these parameters at the "nose" point $\mathbf{r}_N = (0, 0, 90\,AU)$. As we can see from this table that parameters V_x and V_y of primary oxygen are very small, which means that the direction of O_{pr} bulk velocity vector is almost identical to the V_{LISM} direction. The parameter V_y of the secondary oxygen is also very small, but the parameter V_x significantly differs from zero ($\approx -1.6\ km\ s^{-1}$). Thereby, the secondary oxygen bulk velocity vector is rotated in the BV-plane from the V_{LISM} vector to B_{LISM} by $\approx 4°$.

Table 1. Table of primary and secondary oxygen velocity distribution function moments at 90 AU in the "upwind" direction. These parameters were taken from the numerical calculations of the global model.

Component of ISN oxygen	n_O $[\times 10^{-4}\ cm^{-3}]$	V_x $[km\ s^{-1}]$	V_y $[km\ s^{-1}]$	V_z $[km\ s^{-1}]$	T_x [K]	T_y [K]	T_z [K]
Primary	0.272	-0.006	0.001	-26.877	6538	6522	6225
Secondary	0.373	-1.619	-0.005	-22.315	15541	6767	93982

To get a deeper understanding of properties of the oxygen flow at 90 AU let us introduce not only the moments of the calculated distribution functions but also its shape. Figure 2 shows $f_z(v_z) = f(V_x, V_y, v_z)$ functions of primary and secondary oxygen at $\mathbf{r}_N$ (or, in other words, the profiles in the "upwind" direction). The value of the $f_z(v_z)$ function is proportional to the amount of atoms that have z-component of velocity equals to v_z. Red curve of the figure 2 clearly shows that the primary oxygen can be fitted well with Maxwell – Boltzmann distribution function with appropriate parameters V_z and T_z. Green curve of the figure 2 presents the $f_z(v_z)$ profile of the secondary oxygen. Here we can see a strongly marked peak of atoms with the velocities $v_z \approx -26\ km\ s^{-1}$ and a wide range of slow atoms with approximately the same amount (hereinafter we will use a notion "plank" of slow atoms). This "plank" demonstrates that secondary oxygen component contains atoms that have a smaller velocities than the primary

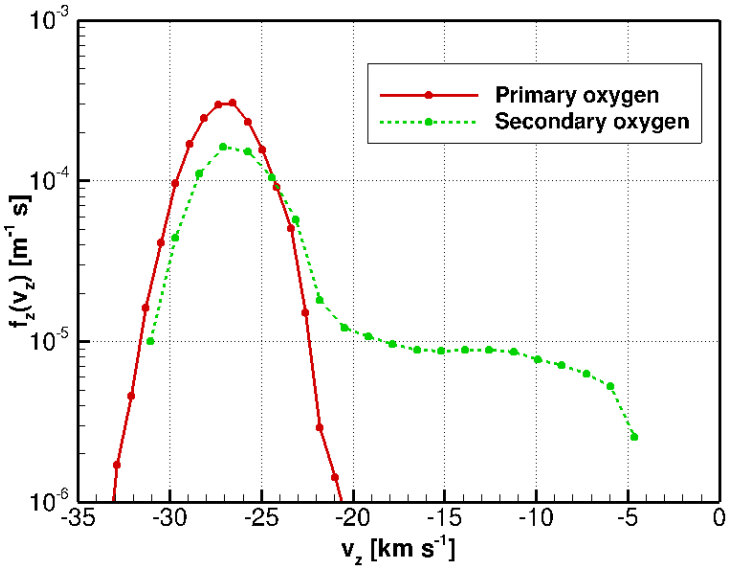

Figure 2. Profiles $f_z(v_z) = f(V_x,\, V_y,\, v_z)$ of the velocity distribution functions of the O_{pr} (red curve) and O_{sec} (green dashed curve) at $\mathbf{r}_N$ in the "upwind" direction. First profile is nearly a Maxwell - Boltzmann distribution function with parameters $(V_z,\, T_z)$ for primary oxygen from table 1. Second profile has two main features: (a) a strongly marked peak of atoms with the velocities $v_z \approx -26\, kms^{-1}$; (b) a "plank" of slow atoms with velocities $-20 < v_z < -5\, km\, s^{-1}$.

ones. These slow atoms are created during charge exchange from O^+ ions decelerated near the heliopause. Oxygen atoms have small thermal velocities that is why all decelerated atoms with different velocities create such kind of "plank" on the total velocity distribution. This feature is absent for the secondary hydrogen atoms because they have much larger thermal velocities and the effect is suppressed.

Therefore, the velocity distribution function of secondary oxygen has a strong non-Maxwellian properties in the region near the TS. The charge exchange process in the heliosheath is responsible for these properties because it leads to disturbances of interstellar oxygen flow. A high value of T_z temperature (see table 1) also indicates that the $f_z(v_z)$ profile can not be properly fitted using a Maxwell – Boltzmann distribution function. Thereby, in the case of secondary oxygen it is necessary to use a specific form of velocity distribution function at 90 AU that takes into account the influence of the heliospheric interface.

As the next step we perform a fit of the velocity distribution functions of primary and secondary oxygen at 90 AU and present formulas of boundary distribution functions $f_s(\mathbf{v}_s)$ that we use in our numerical calculations. We start from the assumption that components $(v_x,\, v_y,\, v_z)$ of vector $\mathbf{v}_s$ (atom velocity at 90 AU) are independent random variables, so the boundary velocity distribution function can be written in general form as:

$$f_s(\mathbf{v}_s) = n_O \cdot f_x(v_x) \cdot f_y(v_y) \cdot f_z(v_z), \quad \int_{-\infty}^{+\infty} f_i(v_i) \cdot dv_i = 1, \tag{6}$$

where $i \in \{x, y, z\}$, n_O is the number density of oxygen (primary or secondary). We assume $f_x(v_x)$ and $f_y(v_y)$ to be Maxwell – Boltzmann distributed with parameters $(V_x,\, T_x)$ and $(V_y,\, T_y)$, respectively:

$$f_i(v_i) = \frac{1}{\sqrt{\pi} c_i} \cdot exp\left(-\frac{(V_i - v_i)^2}{c_i^2}\right),\; c_i = \sqrt{\frac{2k_B T_i}{m}},$$

where $i \in \{x, y\}$. Parameters (V_x, T_x) and (V_y, T_y) and number density n_O of O_{pr} and O_{sec} were derived from the calculations of the global model and presented in table 1.

For primary oxygen we also assume $f_z(v_z)$ to be Maxwell – Boltzmann distributed with parameters (V_z, T_z), which were taken from table 1 as well. For secondary component of neutral oxygen atoms we use the velocity distribution function obtained numerically in the frame of the global model. The $f_z(v_z)$ factor in equation 6 mainly describes a non-Maxwellian properties of the secondary oxygen flow at 90 AU, so we use calculated values of the distribution function and a linear interpolation between them (green curve of the figure 2).

3. Calculation of the model fluxes at 1 AU

In this section we briefly describe the method of calculation of the model fluxes. Using the velocity distribution function we can calculate its integral characteristic, namely, an atom flux at 1 AU in a specified viewing direction. Every position of observer at 1 AU in the ecliptic plane can be defined by its ecliptic (J2000) longitude λ_{obs}. Plane of observations is perpendicular to a Sun – observer vector and can be consequently defined by its direction. This geometry of observations is similar to the IBEX observations. Line of sight (LOS), which lies in the observational plane, can be defined by only one angle and, for instance, it can be a α_{NEP}-angle that counted from the north ecliptic pole (NEP). Thereby, the flux at 1 AU in specified line of sight $\mathbf{S}_{LOS}$ can be calculated by the following formula:

$$Flux = \int_0^{+\infty} f(\mathbf{r}, \mathbf{v}, t) \cdot v^3 \cdot dv, \ \mathbf{v} = -v \cdot \mathbf{S}_{LOS},$$

where $[Flux] = s^{-1}cm^{-2}sr^{-1}$ and $\mathbf{v}$ is the absolute atom's velocity, which direction is determined by the LOS.

To calculate the model fluxes we use the following algorithm. A full sky map in ecliptic (J2000) coordinates $\{(\lambda, \beta) \in [0°, 360°] \times [-90°, 90°]\}$ was divided into $2° \times 2°$ bins in a form of 2D array. Thus, every bin is defined by the pair of indexes (i, j), where $i \in [0, 179]$ and $j \in [0, 89]$. By a specified longitude of observer λ_{obs} and a given value of α_{NEP} we can clearly define LOS and a bin of the sky map to which it belongs.

Total flux $F(i, j)$ in the (i, j)-bin was averaged over one year. As we have mentioned in the Section 2, the simplified ionization model with constant ionization rate was used in the present work, therefore the distribution function $f(\mathbf{r}, \mathbf{v}, t)$ and the value of the flux do not depend on time t. Thus, it does not matter what year is chosen for averaging of the flux $F(i, j)$. Simulations were performed for the lines of sight characterized by $\lambda_{obs} \in [0°, 360°]$ and $\alpha_{NEP} \in [0°, 360°]$ with steps of 1° (further steps reduction does not substantially change the value of the flux).

4. Results of the model numerical calculations

The results of the numerical calculations are presented in figure 3 in a form of the flux maps at 1 AU. The numerical calculations were performed for each sort of oxygen atoms separately: plot 3(A) presents fluxes of the primary oxygen and plot 3(B) presents fluxes of the secondary oxygen.

There are two peaks in the figure 3(A) that are obtained in the following directions of the sky map: $(\lambda_1, \beta_1) \approx (220°, 5°)$ and $(\lambda_2, \beta_2) \approx (290°, 5°)$. Due to the influence of the solar gravitational force the flow of oxygen atoms changes its direction, so these peaks in the flux map correspond to the opposite directions of the atoms flow at 1 AU. According to this figure, the primary oxygen flow at 1 AU is shifted by $\approx 35°$ from the "upwind" direction ($\lambda_{upwind} = 255.4°$). The symmetry of these two peaks is the result of the fact that $f_x(v_x)$ and $f_y(v_y)$ boundary functions of the primary oxygen at 90 AU are quite simillar (parameters (V_x, T_x) and (V_y, T_y) of these functions are about the same, see table 1).

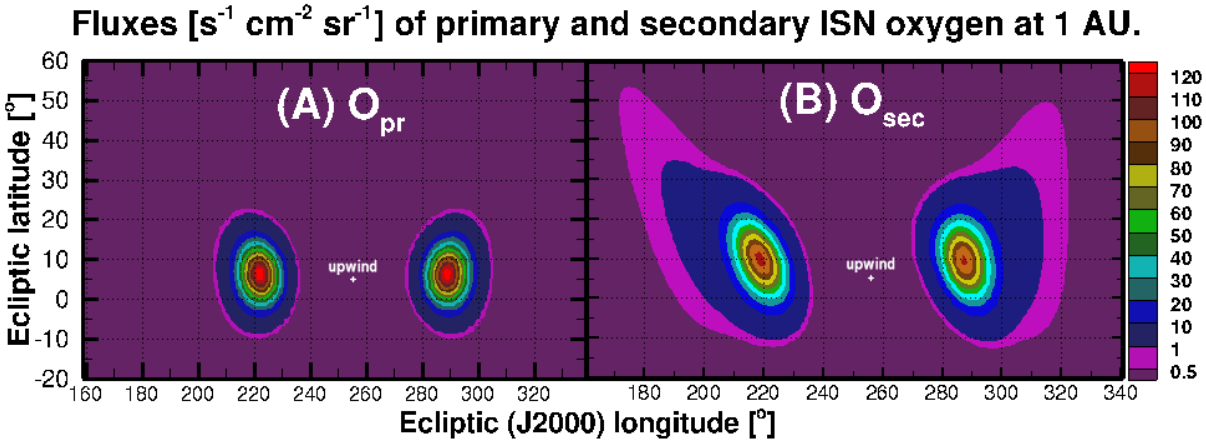

Figure 3. Numerical flux maps at 1 AU in the ecliptic (J2000) coordinates. Boundary conditions are based on the results of numerical calculations of the global model of SW/LISM interaction. Figure (A) presents fluxes of the primary oxygen, figure (B) presents fluxes of the secondary oxygen.

The O_{sec} flux map qualitatively differs from the O_{pr} flux map: on the one hand, there are also two visible peaks in figure 3(B), but on the other hand, these peaks have strongly pronounced "tails" and there is asymmetry between them. The left peak has a "tail" that lays in the region of the lower longitudes and higher latitudes from the main flow and the right "tail" lays in the region of the higher longitudes and higher latitudes. These "tails" are the product of the "plank" of slow atoms of the boundary function $f_z(V_z)$, which is discussed in Section 2.3 (see green curve of the figure 2). The asymmetry of the peaks in O_{sec} sky map of fluxes corresponds to the difference between the $f_x(v_x)$ and $f_y(v_y)$ boundary function of the secondary oxygen (see table 1). The structure of the "tails" strongly depends on the parameters of the boundary function $f_s(\mathbf{v}_s)$ and study of this dependence is beyond the scope of this paper.

The flux sky maps provided by IBEX contain only one visible "tail", which corresponds to the left one of the figure 3(B), due to the fact that these maps were obtained in the spacecraft reference frame. Nevertheless, according to the numerical modelling we can make a conclusion that the extended "tail" in IBEX data correspond to the decelerated and heated secondary oxygen population.

5. Summary and conclusions

In this work we have studied the distribution of the ISN oxygen atoms in the heliosphere and its fluxes at Earth's orbit. The main points of this work are:

(i) An advanced kinetic model that takes into account the secondary component of the interstellar neutral oxygen atoms was provided.

(ii) Numerical modelling of the ISN O (primary and secondary) fluxes at Earth's orbit was performed.

(iii) According to the results of the numerical calculations, we can make a conclusion that the extended "tail", which is observed in the IBEX data, is a product of the secondary component of ISN oxygen atoms, thereby the results of this work support the Park et al. [7] assumption that the "tail" is connected with the secondary oxygen population.

To perform a quantitative comparison between the IBEX data and numerical calculations we need to transform the model fluxes into the IBEX count rates. The method of transformation

should make allowance for the motion and geometry of IBEX spacecraft observations, all technical features of the IBEX-Lo sensor and the results of its calibration. The matter of the future investigations is to consider all of these aspects and to perform a detail quantitative comparison of the results of numerical modelling with the IBEX data.

Acknowledgments

Work is supported by Program 7 of Presidium RAS (in part of studying of oxygen distribution in the heliosphere). Calculations of ISN oxygen distribution were performed by using the Supercomputing Center of Lomonosov Moscow State University.

References

[1] McComas D J, Bzowski M, Frisch P, Fuselier S A, Kubiak M A, Kucharek H, Leonard T, Möbius E, Schwadron N A, Sokół J M, Swaczyna P and Witte M 2015 *The Astroph. J.* **801** 28
[2] Izmodenov V V, Malama Y G, Gloeckler G and Geiss J 2004 *Astron. & Astroph.* **414** L29–L32
[3] Izmodenov V V, Malama Y G and Lallement R 1997 *Astron. & Astroph.* **317** 193–202
[4] Izmodenov V V, Lallement R and Geiss J 1999 *Astron. & Astroph.* **344** 317–321
[5] Geiss J, Gloeckler G, Mall U, von Steiger R, Galvin A B and Ogilvie K W 1994 *Astron. & Astroph.* **282** 924–933
[6] Cummings A C, Stone E C and Steenberg C D 2002 *The Astroph. J.* **578** 194–210
[7] Park J, Kucharek H, Möbius E, Galli A, Livadiotis G, Fusellier S A and Mccomas D J 2015 *The Astroph. J. Suppl. Ser.* **220** 34
[8] Izmodenov V V, Katushkina O A, Qumerais E and Bzowski M 2013 *Cross-Calibration of the Far UV Spectra of Sloar System Objects and the Heliosphere* ISSI Scientific Report Series vol 13 ed E Qumerais and M Snow et al (Bern:ISSI) p 7
[9] Katushkina O A, Izmodenov V V, Wood B E and McMullin D R 2014 *The Astroph. J.* **789** 80
[10] Katushkina O A, Izmodenov V V, Alexashov D B, Schwadron N A and Mccomas D J 2015 *The Astroph. J. Suppl. Ser.* **220** 33
[11] Izmodenov V V 2006 *The Physics of the Heliospheric Boundaries* ed. V V Izmodenov & R Kallenbach (ESA Publications Division, EXTEC) p 45
[12] Bzowski M, Sokół J M, Kubiak M A and Kucharek H 2013 *Astron. & Astroph.* **557** A50
[13] Izmodenov V V and Alexashov D B 2015 *The Astroph. J. Suppl. Ser.* **220** 32
[14] Witte M 2004 *Astron. & Astroph.* **426** 835–84
[15] Lallement R, Quemerais E, Bertaux J L, Ferron S, Koutroumpa D and Pellinen R 2005 *Sci.* **307** 1447–49